

# We are IntechOpen, the world's leading publisher of Open Access books Built by scientists, for scientists

## 4,800

Open access books available

## 122,000

International authors and editors

## 135M

Downloads

Our authors are among the

## 154

Countries delivered to

## TOP 1%

most cited scientists

## 12.2%

Contributors from top 500 universities

**WEB OF SCIENCE™**Selection of our books indexed in the Book Citation Index  
in Web of Science™ Core Collection (BKCI)

Interested in publishing with us?  
Contact [book.department@intechopen.com](mailto:book.department@intechopen.com)

Numbers displayed above are based on latest data collected.

For more information visit [www.intechopen.com](http://www.intechopen.com)

# Application of Piezoelectric Transducers in Structural Health Monitoring Techniques

Najib Abou Leyla<sup>1</sup>, Emmanuel Moulin<sup>1</sup>, Jamal Assaad<sup>1</sup>,  
Farouk Benmeddour<sup>1</sup>, Sébastien Grondel<sup>1</sup> and Youssef Zaatara<sup>2</sup>

<sup>1</sup>*Department of OAE, IEMN, UMR CNRS 8520, Université de Valenciennes  
et du Hainaut Cambrésis, Le Mont Houy,*

<sup>2</sup>*Applied Physics Laboratory – Lebanese University – Campus,*

<sup>1</sup>*France*

<sup>2</sup>*Lebanon*

## 1. Introduction

The technological advances of recent years have contributed greatly to the prosperity of the society. An important element of this prosperity is based on networks of inland, sea, and air transports. However, security in all transport networks remains a major challenge. More specifically, many researches in the field of aeronautics were done to increase the reliability of aircrafts. The themes of NDT (Non Destructive Testing), and more precisely the concept of SHM (Structural Health Monitoring), have thus emerged.

The SHM is a technical inspection to monitor the integrity of mechanical structures in a continuous and autonomous way during its use. Sensors used in this technique being fixed and/or integrated to the structure, it differs from traditional NDT using mobile probes. The first issue is obviously security; a second important issue is reducing financial costs of maintenance. Thus, a new technique that increases reliability and decreases costs of maintenance at the same time seems to be a technological revolution.

Indeed, the traditional inspection methods require planned interventions, and periodic detention of the aircraft, and in some cases the dismantling of some parts. This entire procedure is necessary despite the high costs incurred. Added to that financial aspect, the risk of the occurrence of an unscheduled technical problem between two scheduled inspections is possible. Such a scenario may lead to the replacement of some parts often costly, and fortunately in less frequent cases to air disasters.

## 2. Background work and contributions of the team

Security in aeronautics being a major issue, regular inspections is needed for maintenance. In fact, these materials are subjected to harsh conditions of operation that may damage them, and thus affect security. Nowadays, traditional inspections induce long immobilization of the aircraft and therefore high costs.

A research project aimed at developing a SHM system based on guided elastic waves and applicable to aeronautic structures has been elaborated by our laboratory. We sought to understand the propagation of ultrasonic waves in the structures, their interaction with damage, and the behavior of different type of sensors. This global vision aims at increasing the reliability of the inspections while decreasing maintenance costs. For this purpose, embedding the transducers to the structure seems to be interesting. Indeed, ultrasonic waves present in the material, called Lamb waves, spread over long distances and interact with damages present in the structure. Their damage detection capabilities has been known for a long time [1,2]. By implanting small piezoelectric transducers into the structures, Lamb waves can be emitted and received and it is theoretically possible to monitor a whole given area [3,4].

Over the last 15 years, the team has therefore studied the different axes of the SHM:

- Characterization of wave propagation in aeronautic materials
- Interaction of ultrasonic waves with damage
- The use of different type of sensors
- Behavior modeling of transducers
- Development of adapted processing tools

The expected benefits of SHM system can thus be summarized in few points:

- Optimization of maintenance plans (decrease immobilisation periods and therefore maintenance costs)
- Increase security (more frequent inspections in an almost real-time)
- Increase the life duration of an aircraft

The theme of SHM started in our team for fifteen years with the researches of Blanquet [5] and Demol [6]. These works were devoted respectively to the study of the propagation of the Lamb waves and the development of multi-elements transducers to generate and receive this type of waves in a material. In the continuity of these researches, E. Moulin has studied the Lamb wave generation [7, 8, 9] and has developed a technique [10] allowing the prediction of the Lamb wave field excited in an isotropic plate by a transducer of finite dimensions. In another work [11], a simple and efficient way of modeling a full Lamb wave emission and reception system was developed. Other works have treated the question of Lamb wave emission and/or reception using thin, surface-bonded PZT transducers. Giurgiutiu [12] has used a “pin force” model to account for the mechanical excitation provided by the emitter. Then, the response of the plate in terms of Lamb waves excitation has been derived analytically in a 2D, plane strain situation. Nieuwenhuis et al [13] have obtained more accurate results by using 2D finite element modeling, which allows a better representation of the transducer behavior. Lanza di Scalea et al [14] have focused on the reception of unidirectionally propagating, straight-crested Lamb or Rayleigh waves by a rectangular transducer.

S. Grondel [15] has optimized the SHM using Lamb waves for aeronautic structures by studying the adapted transducer to generate Lamb waves. Paget [16] has elaborated a technique to detect damage in composite materials. In another work, Duquenne [17] has implemented a hybrid method to generate and receive Lamb waves using a glued-surface transducer in a transient regime. F. El Youbi [18] has developed a sophisticated signal

processing technique based on the frequency-time technique and the Fourier transform spatiotemporal to study separately the sensibility of each Lamb mode to damage. More recently F. Benmeddour [19, 20] has studied the interaction of Lamb waves with different type of damage by modelling the diffraction phenomena, and M. Baouahi [21] has considered the 3-D aspect of the Lamb waves generation.

A wide range of work has already been reported on the interaction of Lamb waves with damage and discontinuities such as holes [22, 23], delaminations [24, 25], vertical cracks [26], inclined cracks [27], surface defects [28], joints [29, 30] and thickness variations [31]. More specifically, studies of the interaction with notches have also been carried out. For example, Alleyne et al. [32, 33], have studied the sensitivity of the A0, S0 and A1 modes to notches. In this analysis, they have shown the interest of using the two-dimensional Fourier transform to quantify each scattered Lamb mode. More recently, Lowe et al. [34, 35], have analyzed the behavior of the A0 mode with notches as a function of the width and the depth. The authors [36] have then extended this study to the S0 mode.

Finally, E. Moulin [37] studied and validated experimentally the potential of developing a passive SHM system (without the need on an active source), based on the exploitation of the natural ambient acoustic sources present in an aeronautic structure during flight. This technique has been widely exploited in seismology [38, 39, 40], underwater acoustics [41, 42] and recently ultrasonic [43, 44, 45].

These works contributed to the progress of resolving the different problems related to SHM. They can be synthesized in four main points:

- The modeling of an active complete SHM system (transmission / propagation / reception), in the absence of damage: Development of an efficient modeling tool that takes into account the actual characteristics, including 3-D aspect
- The modeling and interpretation of diffraction phenomena (transmission, reflection, mode conversions) on a number of defect types
- Development of a sophisticated signal processing technique (time-frequency technique and spatiotemporal Fourier transform) to minimize the risk of misinterpretation
- Demonstration of the feasibility of a passive SHM system based on the exploitation of natural ambient acoustic fields.

All of this work has enabled the team to acquire the skills needed to develop a SHM system. The following section is devoted to the presentation of some results for each of the above points.

### 3. Modeling and results

#### 3.1 Modeling of emission – reception transient system

The work described in this section is intended to present a simple and efficient way of modeling a full Lamb-wave emission and reception system. The advantage of this modular approach is that realistic configurations can be simulated without performing cumbersome modeling and time-consuming computations. Good agreement is obtained between predicted and measured signals.

It will be assumed here that the bonded piezoelectric receiver has a small influence on the wave propagation [46]. As a consequence, the displacement imposed at the plate-receiver interface will be considered to be the surface displacement field associated to the incident Lamb waves. The validity of this assumption is realistic if either the transducer is very thin compared to the plate thickness or very small compared to the shortest wavelength [11].

The emission process is modeled using the finite element - normal mode technique described above. It allows predicting the modal amplitudes of each Lamb mode. Then, each Lamb mode is treated separately as a displacement input on the lower surface of the receiving transducer. In summary, the input of the model is the electrical signal (in volts) applied to the emitter and the output is the electrical signal (in volts) received at the receiver. Therefore, the theoretical and measured results can be directly compared to each other, without any adjustment parameters.

Two experimental configurations have been tested. In each case, two parallelepiped-shaped piezoelectric transducers have been glued on the upper surface of a 6-mm thick aluminum plate. One of them is 3-mm wide, 500- $\mu\text{m}$  thick and 2-cm long and is used as the emitter. In the case which will be referred to as setup #1, the receiver is 3-mm wide, 200- $\mu\text{m}$  thick, 2-cm long and has been placed 20 cm away from the emitter. In setup #2, the emitter-receiver distance is 15 cm and the receiver is 0.5-mm wide, 1-mm thick and 2-cm long (figure 1). This choice for the dimensions of the receivers has been guided by the assumption discussed above.

The electric excitation signal is provided by a standard waveform generator with output impedance 50  $\Omega$ . The signal received at the second transducer is directly measured, without any amplification or filtering, using a digital oscilloscope with sampling rate 25 Ms/s and input impedance 1 M $\Omega$ . The lateral dimensions of the plate have been chosen large enough as for avoiding parasitic reflections mixed with the useful parts of the received signals. The frequency range considered for the study spreads from 100 to 500 kHz.

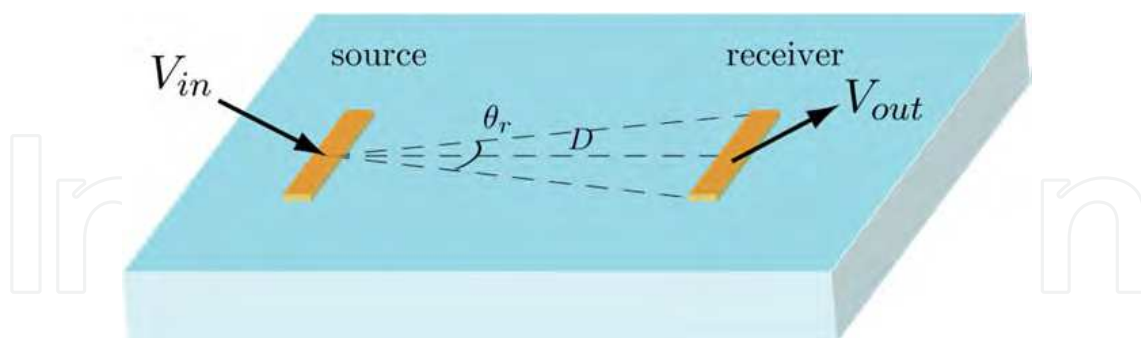


Fig. 1. Source - receiver configuration. Three-dimensional, realistic situation

The first example, presented in figure 2, corresponds to setup #1 where the emitter is excited with an input signal  $V_{in}$  which is a 5-cycle, 10 V amplitude, Hanning-windowed sinusoid signal with central frequency 450 kHz. The received signal is an electric voltage  $V_{out}$ . In this case, the first three Lamb modes  $A_0$ ,  $S_0$  and  $A_1$  are expected.

The measured and predicted waveforms (Fig. 2-a and -b, respectively) appear to be in good agreement. The three main wave packets, corresponding to the three generated Lamb modes, are clearly visible.

The second example corresponds to the results obtained for setup #2, with excitation frequency 175 kHz (Fig. 3). Comments very similar as above can be made. Here again, both the absolute amplitudes as well as the global waveforms are correctly predicted.

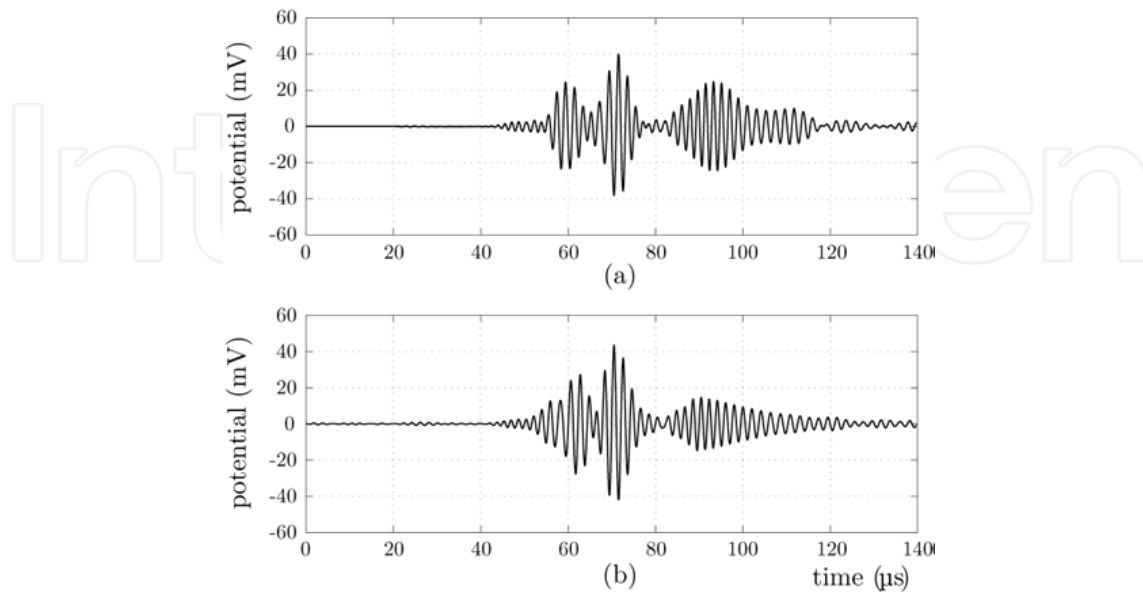


Fig. 2. Electrical potential at the 3-mm wide, 0.2-mm thick receiver (setup #1), for a 450 kHz excitation. (a) Experimental. (b) Predicted.

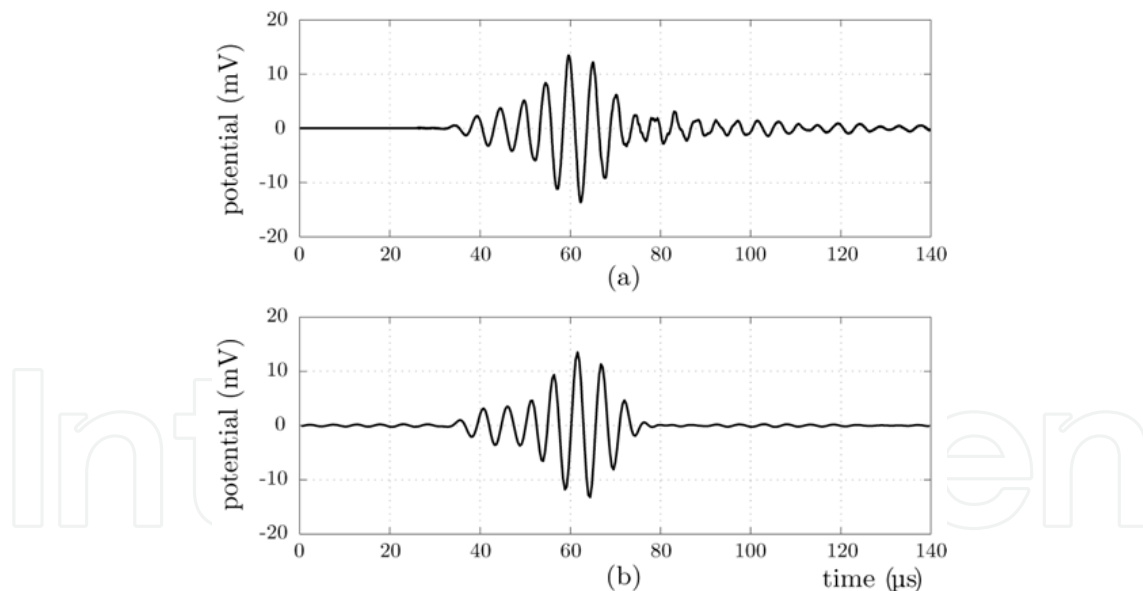


Fig. 3. Electrical potential at the 0.5-mm wide, 1-mm thick receiver (setup #2), for a 175 kHz excitation. (a) Experimental. (b) Predicted.

### 3.2 Fundamental Lamb modes interaction with symmetrical and asymmetrical discontinuities

The aim of the work presented in this section is to predict the propagation of the fundamental Lamb modes in a structure containing symmetrical [19] and asymmetrical [20] discontinuities in a simple and a fast way. The key point is to decompose a given damage

into two elementary types; the symmetrical damage with respect to the median plane and the asymmetrical one in the plate section. The power reflection and transmission coefficients are computed, using two techniques, the finite element method with the help of the Atila code, and the average power flow equation. Indeed, the characterization of damage is done from the average flow of power. It allows determining the power reflection and transmission coefficients.

To calculate these coefficients, normal and tangential displacements, as well as the stresses throughout the plate thickness are needed. It is experimentally impossible. While the developed method, based on the decomposition of normal modes, allows the calculation of the average power flow from only a normal displacement or a tangential one acquired at the surface of the plate. The advantages of this technique are that the time processing of the data is reduced, and it allows a direct comparison with the experimental measurements.

To validate the numerical results, the following experimental study was carried out. The instrumentation used in the experimental investigation is shown schematically in the fig. 4. A pulse, from the pulse generator (HM 8035), is used to simultaneously trigger the oscilloscope (Le Croy type LT344) and the two arbitrary function generators (HP 33120A) that deliver a tone burst modified by a Hanning window function to the transducers. The central frequency is taken equal to 200 kHz. The incident Lamb wave of a specific mode is launched by means of two identical piezo-ceramic transducers (PZT-27) placed at the opposite sides of the plate edge. The thickness, the width and the length of these transducers are equal to 1, 6 and 50 mm, respectively. The free lateral resonance frequency of these transducers is near to 200 kHz. The generation of the A0 mode is obtained by exciting the two thin piezo-ceramic transducers with anti-phased electrical signals. On the contrary, the in-phased excitation generates the S0 mode. Two conventional Panametrics transducers are placed on the plate surface before and after the notch. Local honey and gel coupling are employed for the emitters and receivers, respectively. All the signals from the sensors are then recorded using a digital oscilloscope and transferred via the GPIB bus to a computer for signal processing. The aluminum plate used in the experimental investigations is considered with thickness ( $2d$ ) and length ( $2L$ ) equal to 6 and 500 mm, respectively. The longitudinal velocity (CL), the transverse velocity (CT) and the density ( $\rho$ ) of this plate are equal to 6422, 3110 m/s and 2695 kg/m<sup>3</sup>, respectively. The plate is considered lossless. Here, the notch has a variable width equal to  $w$ . The plate thickness changes abruptly either from  $2d$  to  $2dp$  or from  $2dp$  to  $2d$ , with  $d$  the half thickness of the plate and  $p$  takes values from 0 to 1 with a constant increment.

In this work, the fundamental Lamb mode, S0 or A0, is launched from the plate edge. The generation of the S0 mode is performed by the application, at the left edge of the plate, of both tangential symmetrical and normal anti-symmetrical displacements, with respect to the median plane, windowed by Hanning temporal function. Alternatively, the generation of the A0 mode is obtained by the application of the tangential anti-symmetrical and the normal symmetrical displacements.

For the symmetrical notches, no mode conversion is observed, which is consistent with the theoretical symmetry principles. The figure 5 shows the comparison between the reflection and transmission power coefficients obtained when the A0 and S0 modes are launched. We can see a good agreement between the experimental and the numerical results.

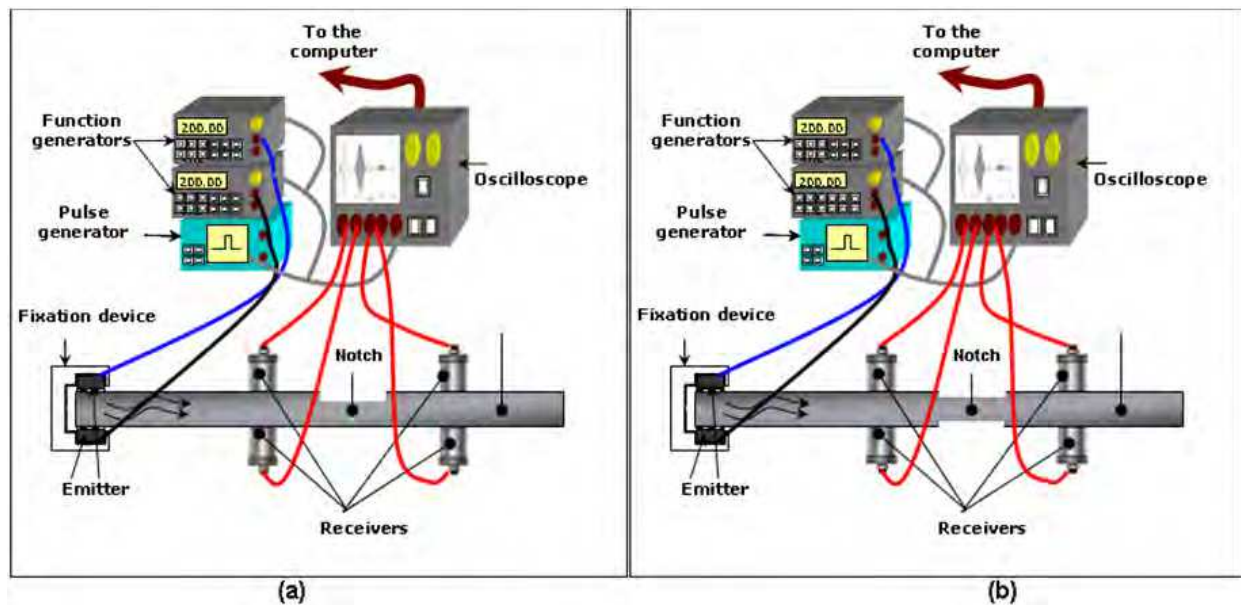


Fig. 4. Experimental device to study the interaction of Lamb modes with (a) asymmetrical discontinuities and (b) symmetrical discontinuities.

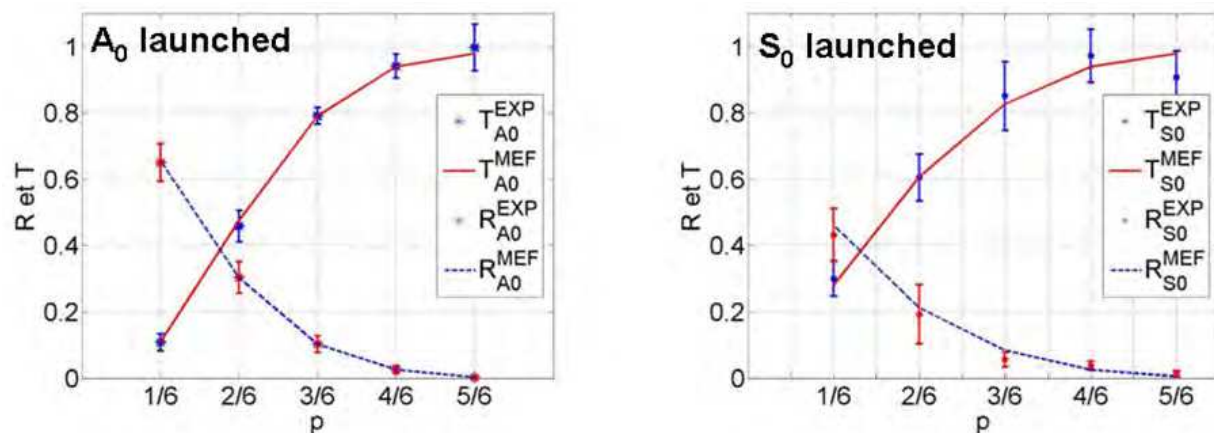


Fig. 5. Comparison between numerical and experimental results for the reflection (R) and the transmission (T) coefficients, when the launched Lamb mode  $A_0$  (a) or  $S_0$  (b) interacts with a symmetrical discontinuity.

For the asymmetrical notches a mode conversion from the incident mode  $A_0$  to the converted mode  $S_0$  and inversely is enabled. The curves of figure 6 show a good agreement between the experimental and the numerical results for the reflection coefficient, for both incident and converted modes, when the  $A_0$  or  $S_0$  mode is launched.

### 3.3 Dual signal processing for damage detection

The identification of Lamb mode amplitude variation as a function of the damage evolution is still the most difficult step in the process of damage monitoring using embedded Lamb wave-based systems. The aim of this section is to propose a simple system based on the generation of two different frequencies in order to better identify Lamb mode amplitude and to avoid false data interpretation in plates containing a hole of variable diameter. This



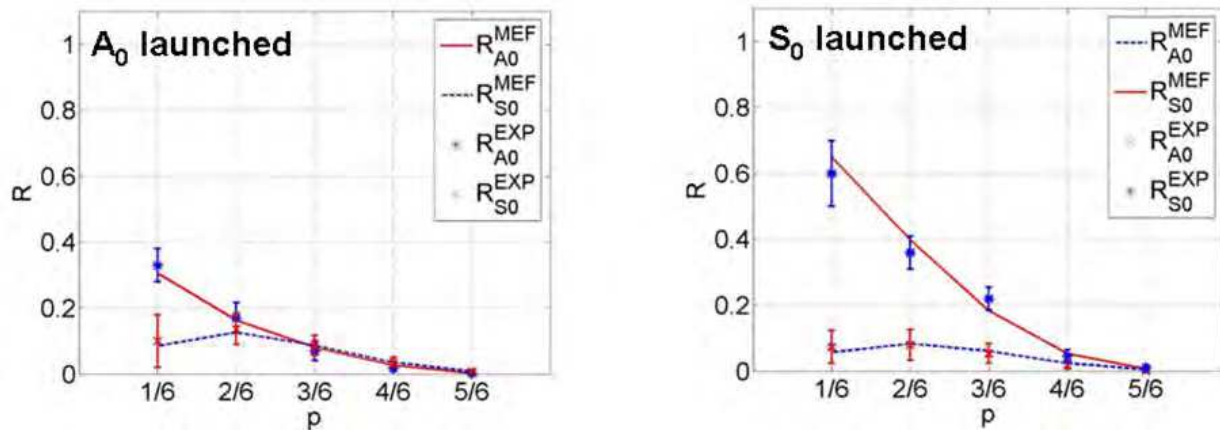


Fig. 6. Comparison between numerical and experimental results for the reflection (R) coefficient, when the launched Lamb mode A<sub>0</sub> (a) or S<sub>0</sub> (b) interacts with an asymmetrical discontinuity.

identification is based on a simple relation between the short-time Fourier transform (STFT) and the two-dimensional Fourier transform (2DFT).

Experimentally, a 3 mm thick aluminum plate with an emitter and a receiver is considered (Figure 7). The emitter consists of two piezoelectric elements with different widths in order to allow the excitation of two different frequency bands. Their sizes were equal to  $15 \times 3 \times 1 \text{ mm}^3$  and  $15 \times 2 \times 1 \text{ mm}^3$ , which correspond to transverse resonance frequencies of 400 kHz and 600 kHz, respectively. The receiver consists of a 32-electrodes piezoelectric transducer with an inter-electrode distance of 2 mm, and  $400 \mu\text{m}$  thick, 15 mm wide and 63 mm long. It was developed especially to increase the received power. The initial distance between the emitter and the sensor was chosen to be 25 cm. The Lamb waves generated by the emitter were received on different electrodes of the sensor. All the signals were then recorded by a digital oscilloscope with a sampling frequency equal to 5 MHz and transferred to a PC where the signal processing, i.e. STFT and 2DFT, could be applied.

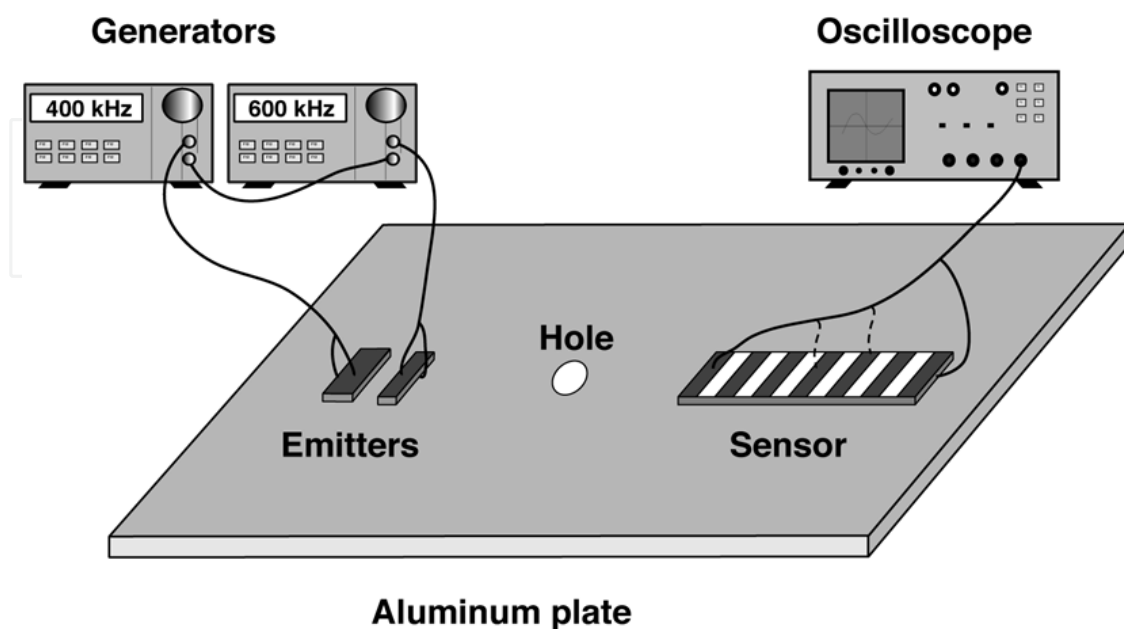


Fig. 7. Experimental measurement setup

In order to simulate the damage, a hole of variable diameter is introduced at the plate centre, and its diameter was increased from 1 mm to 13 mm.

By computing the amplitudes on the 2DFT and STFT analysis as functions of the diameter of the hole, the sensitivity of Lamb modes can be analyzed. In fact, the application of the dual signal processing approach to the received Lamb wave signals allows us to monitor the damage evolution using the  $A_0$  and  $S_0$  Lamb mode amplitude variation in two different frequency bands. Moreover, it is shown (figure 8) that for one of the frequencies a false interpretation can be induced when using only one signal processing technique.

It can be noted that both  $S_0$  and  $A_0$  modes are sensitive to the presence of the hole for both frequencies 400 kHz and 600 kHz, but the interaction of the same mode at different frequencies does not give similar results. At 600 kHz and for both  $S_0$  and  $A_0$  modes (see figures 8(a) and (b)), the amplitudes of the 2DFT and the STFT drop quasi-continuously according to the hole diameter by keeping close values. Both methods give results in good agreement and demonstrate the validity of their use. In contrast to this, in the case of the

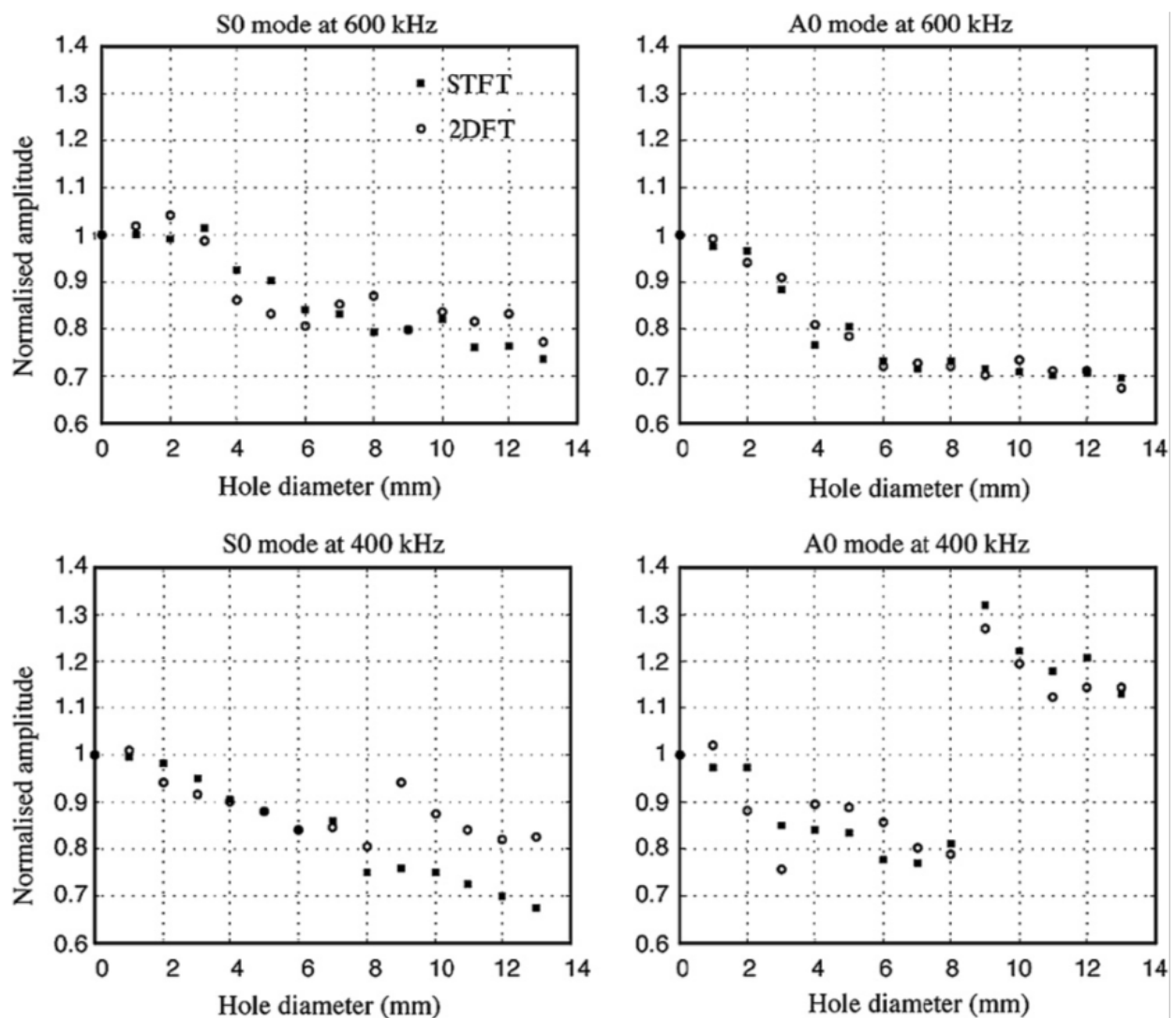


Fig. 8. STFT and 2DFT amplitude variation as a function of the hole diameter. (a)  $S_0$  mode at 600 kHz; (b)  $A_0$  mode at 600 kHz, (c)  $S_0$  mode at 400 kHz; (d)  $A_0$  mode at 400 kHz.

S0 mode at 400 kHz (see figure 8(c)) and for a diameter equal to approximately 9 mm, the amplitude of the 2DFT increases whereas the amplitude of the STFT decreases. Although this variation is relatively small, it represents typically a problem of false data interpretation. Simultaneously, in the case of the A0 mode at 400 kHz (see figure 8(d)), the STFT and the 2DFT amplitudes plotted as functions of the hole diameter show that the amplitudes are considerably increased for a hole diameter greater than 9 mm. Again a false data interpretation can be induced concerning the severity of the damage. This change can be related to a resonance phenomenon related to the presence of the hole. A better understanding of this phenomenon requires three-dimensional studies.

These measurements demonstrate the ability to use the STFT and 2DFT at the same time in order to detect damage and to overcome the problem of false data interpretation. In fact, using only one technique and one frequency can not always allow us to get the severity of the damage and consequently to determine the Lamb wave sensitivities to the presence of damage.

Although the results obtained with the STFT are more satisfactory than the 2DFT in this case, they would be more severe in error if the group velocities of the two modes were more similar or if the tested structure was more complex.

### 3.4 Passive SHM using ambient acoustic field cross-correlation

Recent theoretical and experimental studies have shown the possibility to retrieve the Green function between two points in a structure by cross-correlating the received signals at these points simultaneously, in the presence of a diffuse acoustic field in the medium. The aim of the work presented in this section is to exploit the mechanical vibrations and subsequent elastic wave fields present in an aeronautic structure during the flight. These vibrations being the result of the turbo engines and the aero acoustic phenomena, their random character makes the exploitation complicated. Meanwhile, the non need of an active source in this case, is a very interesting solution from an energy consumption point of view.

In the following, the reproducibility of the cross-correlation function, its potential to detect a defect, and its sensitivity to the source characteristics are studied. In fact, since the measured cross-correlation is used to monitor the integrity of the structure, it has to be reproducible for different measurements done in the same conditions. A second necessary condition to the study is the ability to detect any form of heterogeneity in the structure, using the cross-correlation of the ambient acoustic field. Finally, since the source-position influences the result, it is crucial to avoid misinterpretations by separating changes caused by source motion from those caused by defect appearance.

#### 3.4.1 Reproducibility of the cross-correlation function

To study the applicability of the ambient noise correlation method, experimentation in the laboratory has been set-up in order to verify the reproducibility and the sensitivity of the correlation function to a defect. Thus, an aluminum plate of 2\*1 m<sup>2</sup>-surface and 6mm-thickness has been considered, and two circle PZ27-piezoelectric transducers of 0.5cm-radius and 1mm-thickness have been glued with honey at two positions *A* and *B*. To generate the ambient acoustic noise in the plate, an electrical noise generator has been used, and the signal has been emitted using a circle PZ27-piezoelectric transducer of 1cm-radius

and 1mm-thickness, placed at a position  $O$ . The signals received at  $A$  and  $B$  have been measured and sent to a computer using a GPIB bus (Figure 9).

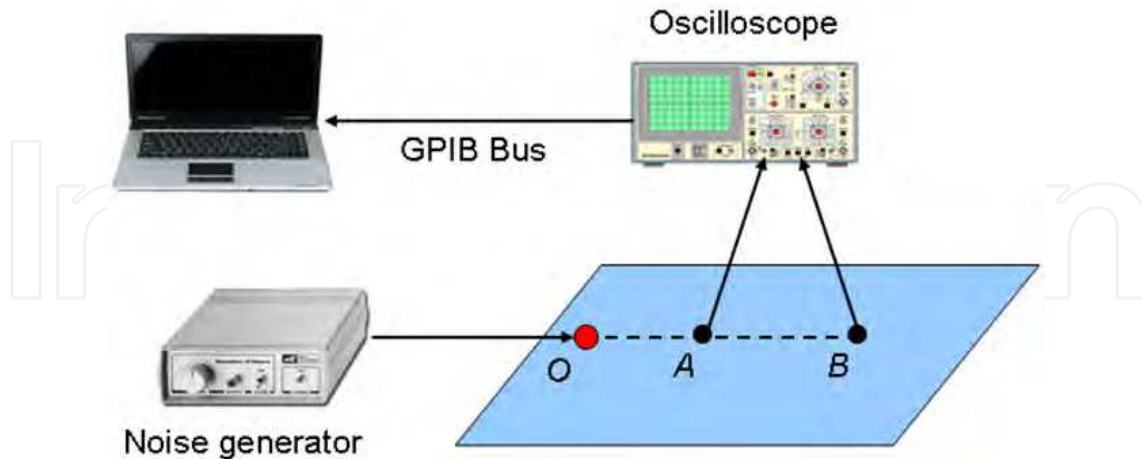


Fig. 9. Experimental set-up for studying reproducibility.

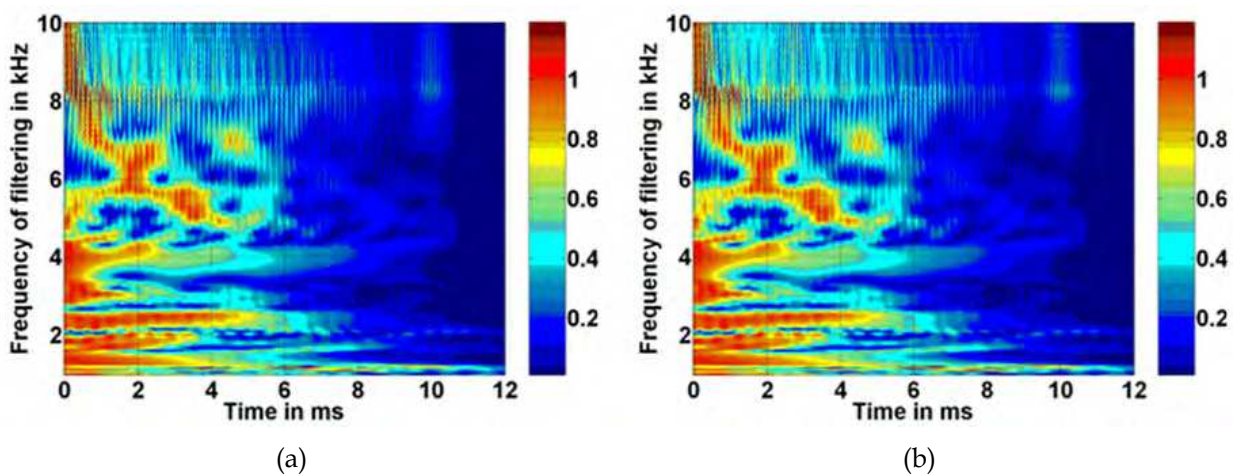


Fig. 10. Cross-correlation function between A and B for the measurement (a) #1 (b) #2.

The cross-correlation between these two signals has then been computed and averaged on  $N = 150$  acquisitions to increase the signal-to-noise ratio. Finally, in order to better analyze the signals, a time-frequency representation has been used. Thus, a wavelet-transform of the measured cross-correlation function has been computed by convolving with a 5-cycle Hanning-windowed sinusoid of variable central frequency  $f_0$ . A time-frequency representation of the cross-correlation function, in the frequency-band [1-6 kHz], is shown at figure 10. We can see that for two measurements done in the same conditions, the cross-correlation function is reproducible.

### 3.4.2 Sensitivity of the cross-correlation function to a defect

In this section, the sensitivity of the cross-correlation function to a defect is studied. Thus, two measurements have been done, one without a defect and the other with a defect somewhere in the plate (Figure 11). Concerning the modeling of the defect, for repeatability purpose, an aluminum disk of 1 cm-radius has been glued on the surface of the plate

between the two points  $A$  and  $B$ . In fact, such a defect introduces local heterogeneity from an acoustic impedance change point of view.

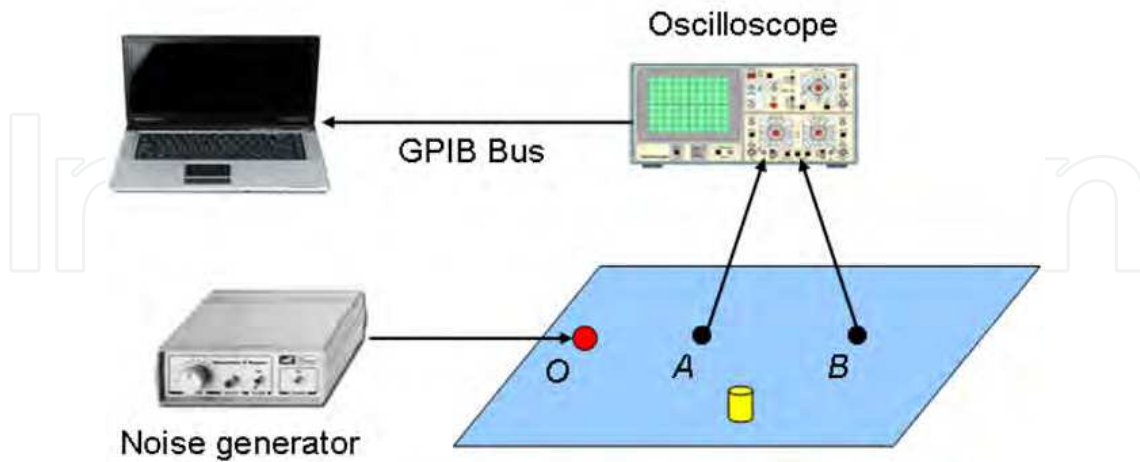


Fig. 11. Experimental set-up for defect detection.

The comparison of the measurements (Figure 12) with and without a defect shows that the cross-correlation function is sensitive to the presence of the defect. The sensitivity is more or less important depending on the frequency range and the position of the defect.

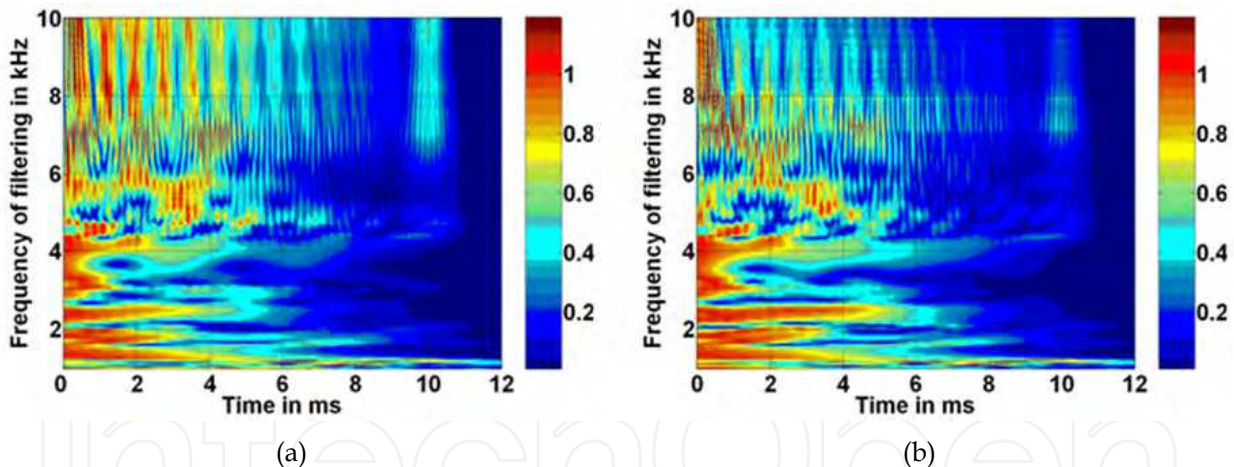


Fig. 12. Cross-correlation function between A and B (a) without and (b) with a defect.

### 3.4.3 Influence of the source characteristics on the cross-correlation function

The reproducibility and the sensitivity to a defect of the cross-correlation function being verified, this section will deal with the study of the influence of the source position on the correlation function. To better highlight the influence of the source position on the cross-correlation function, experimentation with two source positions is done. The images of the figure 13, for the first source position (figure 13.a) and the second source position (Figure 13.b), show that the cross-correlation function depends strongly on the source position. This influence of the source position could be misinterpreted as the appearance of a defect. A solution to this problem is given in the next section.

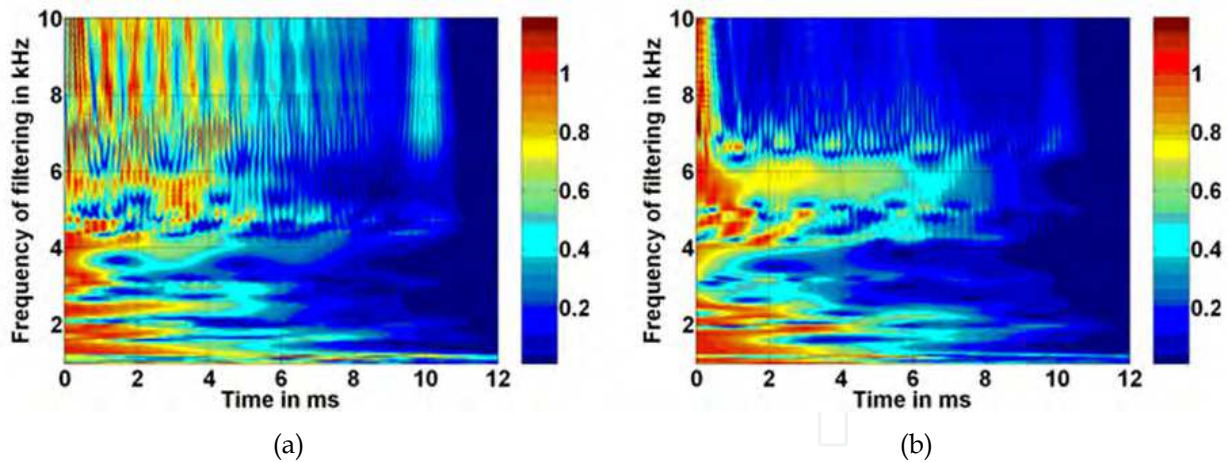


Fig. 13. Cross-correlation function between A and B (a) for the first and (b) for the second source position.

### 3.4.4 Practical application of the ambient noise correlation technique to SHM

In an aeronautic application, the sources exploited can be concentrated and with variable characteristics. This represents a major difficulty for the application. Indeed, in this situation, it is difficult to separate the contributions of the characteristics of the medium, from the characteristics of the source, in the measured information. To overcome this problem, we proposed a solution based on using a third transducer, called “reference transducer” and placed far from A and B, to identify the acoustic source characteristics at the instant of measurement by computing the auto-correlation of the received signal, before doing the diagnostic of the structure.

A simple experimentation has been set-up in the laboratory in order to test the applicability of the principle. Three piezoelectric receivers have been glued, at respective locations A, B and C, on an aluminum plate of  $2\text{ m} \times 1\text{ m}$  surface and 6 mm thickness (Fig. 14). The “ambient” acoustic noise is generated using an amplified loudspeaker working in the audible range (up to approximately 8 kHz), placed under the plate and driven by an electrical noise generator. High-pass filtering is applied in order to reject frequencies below 2 kHz. For repeatability purpose, a “removable” defect was used here instead of an actual structural damage: a small aluminum disk of 1 cm radius bonded between A and B.

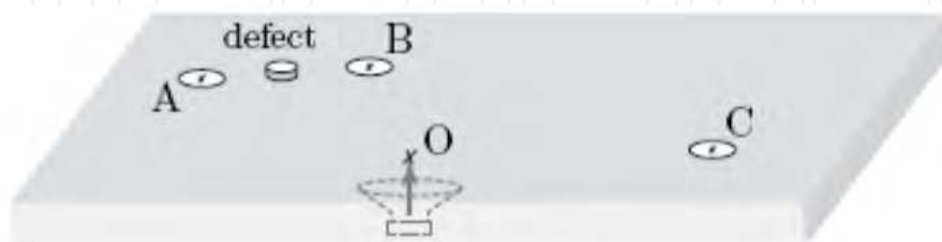


Fig. 14. Description of the experimental setup

The cross-correlation of 0.5 s-long signals measured at positions A and B, and the auto-correlation at position C have been averaged over 150 acquisitions. In order to emphasize interesting effects, narrowband filtering has been applied by convolving it with an N-cycle Hanning-windowed sinusoid of variable central frequency  $f_0$ .

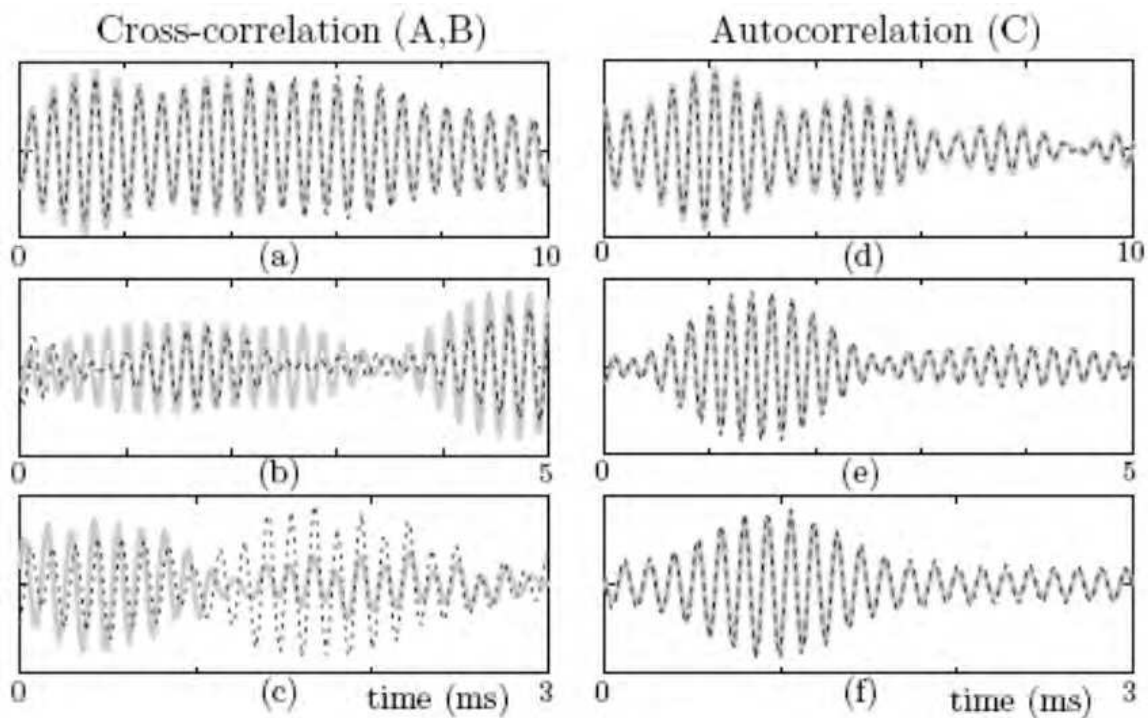


Fig. 15. Filtered average cross-correlation (a, b, c) and autocorrelation (d, e, f) functions with (broken line) and without (solid line) defect. (a), (d)  $f_0 = 2.5$  kHz,  $N = 10$  cycles. (b), (e)  $f_0 = 5.2$  kHz,  $N = 15$  cycles. (c), (f)  $f_0 = 7.8$  kHz,  $N = 15$  cycles.

Thus, comparisons of the results obtained in the absence and in the presence of defect are shown in Fig. 15 for three representative values of  $f_0$ . The curves (a), (b) and (c) show that except in the lower frequency case, the presence of the defect induces significant modifications of the cross-correlation function. As in a typical pitch-catch measurement, amplitude variations as well as phase shifts are observed. Contrariwise, the curves (d), (e) and (f) show that in the same conditions, the auto-correlation at the receiver C is unaffected by the presence of the defect near A and B.

The reliability of the proposed solution depends clearly of the position of the reference receiver C, which should be at the same time not sensitive to the appearance of a defect (in other words far from the inspection area), and sensitive to the source characteristics (close to the source). To quantify more precisely the sensibility of the autocorrelation to the defect and to identify the involved parameters, a theoretic study was done [37].

#### 4. Conclusion

In this paper, a summary of the works developed by our team in the domain of SHM were presented. Thus, the modeling of a complete SHM system (emission, propagation, reception) using finite element method was shown. Then, the study on the interaction of Lamb waves with different types of discontinuities by calculating the power transmission and reflection coefficients was done. In order to better understand this interaction, a dual signal processing based on STFT and 2DFT was presented. This technique allows separating the influence of damage on each Lamb's mode. Finally, a new SHM technique based on the exploitation of the natural acoustic vibration in an aircraft during flight was shown which is

very interesting from an energy consumption point of view. The feasibility of this method was experimentally validated by proposing a solution that allows separating the characteristics of the source and those of the medium. Encouraging results make possible considering the development of autonomous, integrated wireless network sensors for passive SHM application.

## 5. References

- [1] D. C. Worlton, "Ultrasonics testing with lamb waves", *Nondestruct. Test.* 15, 218-222 (1957).
- [2] D. N. Alleyne and P. Cawley, "The interaction of lamb waves with defects", *IEEE Trans. Son. Ultrason.* 39, 381-397 (1992).
- [3] R. S. C. Monkhouse, P. D. Wilcox, and P. Cawley, "Flexible interdigital pvdf lamb wave transducers for the development of smart structures", *Rev. Prog. Quant. Nondestruct. Eval.* 16A, 877-884 (1997).
- [4] J.-B. Ihn and F.-K. Chang, "Detection and monitoring of hidden fatigue crack growth using a built-in piezoelectric sensor/actuator network: I.diagnostics", *Smart Mater. Struct.* 13, 609-620 (2004).
- [5] P. Blanquet, "Etude de l'endommagement des matériaux composites aéronautiques à partir de techniques ultrasonores", PhD Thesis, Report 9724, University of Valenciennes, France (1997).
- [6] T. Demol, "Etude de transducteurs en barettes pour le contrôle santé des structures aéronautiques composites par ondes de Lamb. Application à la caractérisation de l'impact basse vitesse", PhD Thesis, Report 9801, University of Valenciennes, France (1998).
- [7] E. Moulin, J. Assaad, C. Delebarre, H. Kaczmarek and D. Balageas, "Piezoelectric transducer embedded in composite plate : Application to Lamb wave generation," *J. Appl. Phys.* vol. 82, pp 2049-2055 (1997).
- [8] E. Moulin, J. Assaad, C. Delebarre et D. Osmont, "Modelling of Lamb waves generated by integrated transducers in composite plates, using a coupled Finite Element - Normal Modes Expansion method," *J. Acoust. Soc. Am*, vol. 107, pp 87-94 (2000).
- [9] E. Moulin, J. Assaad, C. Delebarre et S. Grondel, "Modeling of integrated Lamb waves generation systems using a coupled finite element - normal modes expansion technique," *Ultrasonics*, vol. 38, pp 522-526 (2000).
- [10] E. Moulin, S. Grondel, M. Baouahi, J. Assaad, "Pseudo-3D modeling of a surface-bonded Lamb wave source", *J. Acoust. Soc. Am.*, vol. 119, pp 2575-2578, 2006.
- [11] E. Moulin, S. Grondel, J. Assaad, L. Duquenne, "Modeling a surface-mounted Lamb wave emission-reception system : Applications to structural health monitoring", à paraître dans *J. Acoust. Soc. Am.*, 2008.
- [12] V. Giurgiutiu, "Tuned lamb wave excitation and detection with piezoelectric wafer active sensors for structural health monitoring", *J. Intell. Mater. Syst. Struct.* 16, 291-305 (2005).



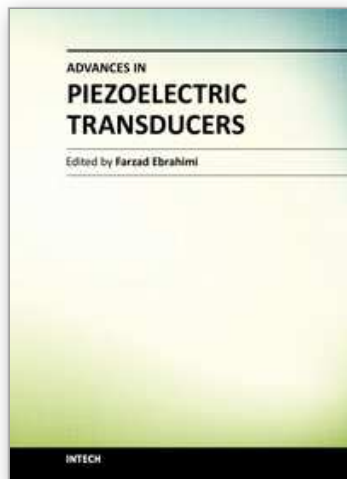
- [13] J. H. Nieuwenhuis, J. J. Neumann, D. W. Greve, and I. J. Oppenheim, "Generation and detection of guided waves using pzt wafer transducers", *IEEE Trans. Ultrason. Ferroelectr. Freq. Control* 52, 2103–2111 (2005).
- [14] F. L. di Scalea, H. Matt, and I. Bartoli, "The response of rectangular piezoelectric sensors to rayleigh and lamb ultrasonic waves", *J. Acoust. Soc. Am.* 121, 175–187 (2007).
- [15] Grondel S, Delebarre C, Assaad J, Dupuis J P and Reithler L, " Fatigue crack monitoring of riveted aluminium strap joints by Lamb wave analysis and acoustic emission measurement techniques" *NDT&E Int.* 25 137–46 (2002)
- [16] C Paget, S Grondel, K Levin, C Delebarre, "Damage assessment in composites by Lamb waves and wavelet coefficients - *Smart Materials and Structures*" 12, p. 393-402, 2003
- [17] L. Duquenne, E. Moulin, J. Assaad, S. Grondel, "Transient modeling of Lamb waves generated in viscoelastic materials by surface bonded piezoelectric transducers", *J. Acoust. Soc. Am*, vol. 116, pp 133-141, 2004.
- [18] El Youbi F, Grondel S and Assaad J. "Signal processing for damage detection using two different array transducers" *Ultrasonics* 42 803–6. (2004)
- [19] F. Benmeddour, S. Grondel, J. Assaad, E. Moulin, "Study of the fundamental Lamb modes interaction with symmetrical notches", *NDT\&E Int.*, vol. 41, pp 1-9, 2007.
- [20] F. Benmeddour, S. Grondel, J. Assaad, E. Moulin, "Study of the fundamental Lamb modes interaction with asymmetrical discontinuities", *NDT\&E Int.*, vol. 41, pp 330-340, 2008.
- [21] M. Baouahi, "Modélisation 3D de la generation des ondes de Lamb par des transducteurs piézoélectriques mono et multi-éléments", PhD Thesis, Report 0711, University of Valenciennes, France (2007).
- [22] Diligent O, Grahn T, Bostro`m A, Cawley P, Lowe MJS. "The low-frequency reflection and scattering of the S0 Lamb mode from a circular through-thickness hole in a plate: finite element, analytical and experimental studies." *J Acoust Soc Am* 2002;112(6):2589–601.
- [23] Grahn T. "Lamb wave scattering from a circular partly through thickness hole in a plate." *Wave Motion* 2003;37:63–80.
- [24] Guo N, Cawley P. "The interaction of Lamb waves with delaminations in composite laminates." *J Acoust Soc Am* 1993; 94(4):2240–6.
- [25] Hayashi T, Kawashima K. "Single mode extraction from multiple modes of Lamb wave and its application to defect detection". *JSME Int J* 2003; 46(4):620–6.
- [26] Le-Cle´zio E, Castaings M, Hosten B. "The interaction of the S0 Lamb mode with vertical cracks in an aluminum plate." *Ultrasonics* 2002; 40:187–92.
- [27] Wang L, Shen J. "Scattering of elastic waves by a crack in a isotropic plate." *Ultrasonics* 1997; 35:451–7.
- [28] Cho Y, Rose JL. "An elastodynamic hybrid boundary element study for elastic wave interactions with a surface breaking defect." *Int J Sol Struct* 2000; 37:4103–24.
- [29] Lowe MJS, Challis RE, Chan CW. "The transmission of Lamb waves across adhesively bonded lap joints." *J Acoust Soc Amer* 2000; 107(3):1333–45.

- [30] Mal AK, Chang Z, Guo D, Gorman M. Lap-joint inspection using plate waves. In: Rempt RD, Broz AL (Eds.), SPIE nondestructive evaluation of aging aircraft, airports, and aerospace hardware, vol. 2945, 1996, p. 128-137.
- [31] Cho Y. "Estimation of ultrasonic guided wave mode conversion in a plate with thickness variation." IEEE Trans Ultrason Ferroelectr Freq Control 2000;17(3):591-603.
- [32] Alleyne DN, Cawley P. "A 2-dimensional fourier transform method for the quantitative measurement of Lamb modes." IEEE Ultrason Symp 1990;1143-6.
- [33] Alleyne DN, Cawley P. "The measurement and prediction of Lamb wave interaction with defects". IEEE Ultrason Sympos 1991; 855-7.
- [34] Lowe MJS, Cawley P, Kao J-Y, Diligent O. "Prediction and measurement of the reflection of the fundamental anti-symmetric Lamb wave from cracks and notches". In: Thompson DO, Chimenti DE, editors. Review of progress in quantitative NDE, vol. 19A. New york: Plenum; 2000. p. 193-200.
- [35] Lowe MJS, Cawley P, Kao J-Y, Diligent O. "The low frequency reflection characteristics of the fundamental antisymmetric Lamb wave A<sub>0</sub> from a rectangular notch in a plate." J. Acoust Soc Am 2002; 112(6):2612-22.
- [36] Lowe MJS, Diligent O. "Low-frequency reflection characteristics of the S<sub>0</sub> Lamb wave from a rectangular notch in a plate". J Acoust Soc Am 2002;111(1):64-74.
- [37] E. Moulin, N. Abou Leyla, J. Assaad, and S. Grondel, "Applicability of acoustic noise correlation for structural health monitoring in nondiffuse field conditions", Appl. Phys. Lett. 95, 094104 (2009).
- [38] N. M. Shapiro, M. Campillo, L. Stehly, and M. Ritzwoller. "High-resolution surface-wave tomography from ambient seismic noise", Science 29, 1615-1617 (2005)
- [39] K. Wapenaar, "Retrieving the elastodynamic Greens function of an arbitrary inhomogeneous medium by cross correlation", Phys. Rev. Lett. 93, 254301 (2004)
- [40] K. G. Sabra, P. Gerstoft, P. Roux, W. Kuperman, and M. C. Fehler "Surface wave tomography using microseisms in southern california", Geophys. Res. Lett. 32, L023155 (2005)
- [41] P. Roux, W. A. Kuperman, and the NPAL Group, "Extracting coherent wavefronts from acoustic ambient noise in the ocean", J. Acoust. Soc. Am. 116, 1995-2003 (2004)
- [42] K. G. Sabra, P. Roux, W. A. Kuperman "Arrival-time structure of the time-averaged ambient noise cross-correlation function in an oceanic waveguide", J. Acoust. Soc. Am. 117, 164-174 (2005)
- [43] K. G. Sabra, E. S. Winkel, D. A. Bourgoyne, B. R. Elbing, S. L. Ceccio, M. Perlin, and D. R. Dowling "Using cross-correlations of turbulent flow-induced ambient vibrations to estimate the structural impulse response. Application to structural health monitoring", J. Acoust. Soc. Am. 121, (4) (2007)
- [44] K. G. Sabra A. Srivastava, F. Lanza Di Scalea, I. Bartoli, P. Rizzo and S. Conti, "Structural health monitoring by extraction of coherent guided waves from diffuse fields", J. Acoust. Soc. Am. 123, (1) (2008)
- [45] E. Larose, P. Roux, and M. Campillo, "Reconstruction of Rayleigh-Lamb dispersion spectrum based on noise obtained from an air-jet forcing", J. Acoust. Soc. Am. 122, (6) (2007)

- [46] L. Duquenne, F. Elyoubi, E. Moulin, S. Grondel, J. Assaad, and C. Delebarre, "The use of permanently-mounted surface transducers to characterize lamb wave propagation", in *Proc. World Congress Ultras.*, 601-604 (Paris, France) (2003).

IntechOpen

IntechOpen



### **Advances in Piezoelectric Transducers**

Edited by Dr. Farzad Ebrahimi

ISBN 978-953-307-931-8

Hard cover, 128 pages

**Publisher** InTech

**Published online** 25, November, 2011

**Published in print edition** November, 2011

The piezoelectric transducer converts electric signals into mechanical vibrations or vice versa by utilizing the morphological change of a crystal which occurs on voltage application, or conversely by monitoring the voltage generated by a pressure applied on a crystal. This book reports on the state of the art research and development findings on this very broad matter through original and innovative research studies exhibiting various investigation directions. The present book is a result of contributions of experts from international scientific community working in different aspects of piezoelectric transducers. The text is addressed not only to researchers, but also to professional engineers, students and other experts in a variety of disciplines, both academic and industrial seeking to gain a better understanding of what has been done in the field recently, and what kind of open problems are in this area.

#### **How to reference**

In order to correctly reference this scholarly work, feel free to copy and paste the following:

Najib Abou Leyla, Emmanuel Moulin, Jamal Assaad, Farouk Benmeddour, Sébastien Grondel and Youssef Zaatari (2011). Application of Piezoelectric Transducers in Structural Health Monitoring Techniques, *Advances in Piezoelectric Transducers*, Dr. Farzad Ebrahimi (Ed.), ISBN: 978-953-307-931-8, InTech, Available from: <http://www.intechopen.com/books/advances-in-piezoelectric-transducers/application-of-piezoelectric-transducers-in-structural-health-monitoring-techniques>

**INTECH**  
open science | open minds

#### **InTech Europe**

University Campus STeP Ri  
Slavka Krautzeka 83/A  
51000 Rijeka, Croatia  
Phone: +385 (51) 770 447  
Fax: +385 (51) 686 166  
[www.intechopen.com](http://www.intechopen.com)

#### **InTech China**

Unit 405, Office Block, Hotel Equatorial Shanghai  
No.65, Yan An Road (West), Shanghai, 200040, China  
中国上海市延安西路65号上海国际贵都大饭店办公楼405单元  
Phone: +86-21-62489820  
Fax: +86-21-62489821

© 2011 The Author(s). Licensee IntechOpen. This is an open access article distributed under the terms of the [Creative Commons Attribution 3.0 License](#), which permits unrestricted use, distribution, and reproduction in any medium, provided the original work is properly cited.

IntechOpen

IntechOpen